Theory of Magnetism of NiF_2

TÔRU MORIYA
Bell Telephone Laboratories, Murray Hill, New Jersey
(Received August 24, 1959)

The magnetic properties of NiF_2 are studied theoretically with the use of a spin Hamiltonian approach. It is shown that the anisotropy of the susceptibility above the Néel temperature indicates a spin arrangement below the Néel temperature in which all the spins are perpendicular to the c axis and the angle between the two sublattice magnetizations is a little smaller than π, giving rise to a small net ferromagnetic moment along the $\langle 100 \rangle$ direction. This model explains the torque data below the Néel temperature quantitatively. The spin wave frequencies and the magnetic resonance frequencies are calculated. There is a low-frequency branch whose lowest frequency ($k=0$) corresponds to the anisotropy energy in the ab plane. The magnetic resonance is expected at around 170 kilomegacycles/second. A recent nuclear magnetic resonance measurement by Shulman seems to support the present model. The spin arrangement below the Néel temperature proposed by Erickson from his neutron diffraction data seems to be neither possible theoretically nor consistent with the other experimental data. Possible structures of domains and domain walls are discussed based on the same model.

1. INTRODUCTION

THE magnetic properties of iron group fluorides, MnF_2, FeF_2, CoF_2, and NiF_2 have been extensively studied both experimentally and theoretically.[1] All of these compounds have a rutile type crystal structure, and the three other than NiF_2 show typical antiferromagnetism below their Néel temperatures; the spins point along the $\pm c$ axes. On the other hand, NiF_2 has been reported to show the following strange properties: It has a weak ferromagnetic moment below its transition point, and the measured torque curves show quite different behavior from those of usual antiferromagnets or those of usual ferromagnets.[2] The specific heat of NiF_2 shows a weaker temperature dependence than those of the other fluorides at low temperatures.[3] A neutron diffraction experiment on a powder sample studied by Erickson[4] led him to conclude that the spins are tilted from the c axis by 10 degrees. These unusual properties have remained unexplained so far. Recently Shulman[5] studied nuclear magnetic resonance of the fluorines in NiF_2. He has come to the conclusion that the spins point in directions almost perpendicular to the c axis, in contradiction with Erickson's analysis of his own neutron diffraction data.

As for the theoretical studies, Dzialoshinski[6] has shown from a symmetry consideration that there are five possible arrangements of the spins in rutile-type crystals assuming a two-sublattice model. Among them are an MnF_2 type structure (the spins pointing in the $\pm c$ directions), structures in which the spins are in the ab plane with a net moment, and a structure proposed by Erickson[4] which, however, is highly improbable even from his argument. His expression for the anisotropy energy is the most general one allowed by the crystal symmetry and some of the terms will vanish in the particular case of NiF_2. A spin Hamiltonian approach, which seems to be adequate for NiF_2, does not give those terms of the anisotropy energy which are expressed by the fourth powers of the spin components or direction cosines of the spins. Kanamori[7] showed from a spin Hamiltonian approach that Erickson's structure is not stable both from classical and quantum-mechanical treatments. There are only two possible arrangements as will be shown in Sec. 4.

The purpose of the present paper is to give a further theoretical study of NiF_2 based on a spin Hamiltonian approach. The main results are as follows: From the anisotropy of the paramagnetic susceptibility we can show that below the Néel temperature the spins align perpendicular to the c axis and there is a net magnetic moment along the a or b axis. This is caused by a rutile-type crystal structure in which there are two kinds of cation sites in a unit cell. This model explains at the same time the torque curves below the Néel temperature; both the magnitudes and the field dependences of the torque curves in the (001) and the (110) planes measured by Matarrese and Stout[2] are explained quantitatively. The nuclear resonance frequencies expected from this model are actually observed recently by Shulman.[5] The spin wave frequency spectra in this model are obtained. There is a branch which starts from the frequency corresponding to an anisotropy energy in the ab plane. This frequency is much lower than the corresponding frequency in usual antiferromagnets, i.e., a geometrical average of the exchange and the anisotropy frequencies. This seems to agree qualitatively with the specific heat data. At the same time the magnetic resonance frequencies for the uniform oscillating field are calculated. There is a mode whose frequency is approximately 170 kilomegacycles/second corresponding

[1] See Nagamiya, Yosida, and Kubo, *Advances in Physics*, edited by N. F. Mott (Taylor and Francis, Ltd., London, 1955), Vol. 4, p. 1. Recently, paramagnetic resonances in samples extremely diluted by ZnF_2, nuclear magnetic resonances, antiferromagnetic resonances, and optical absorption spectra in these iron group difluorides except NiF_2 have been studied by many people, though we don't give references here.
[2] L. M. Matarrese and J. W. Stout, Phys. Rev. **94**, 1792 (1954).
[3] J. W. Stout and E. Catalano, J. Chem. Phys. **23**, 2013 (1955).
[4] R. A. Erickson, Phys. Rev. **90**, 779 (1953).
[5] R. G. Shulman (to be published).
[6] I. E. Dzialoshinski, J. Exptl. Theoret. Phys. U.S.S.R. **33**, 1454 (1959) [translation: Soviet Phys. JETP **6**, 1120 (1958)].
[7] J. Kanamori (unpublished).

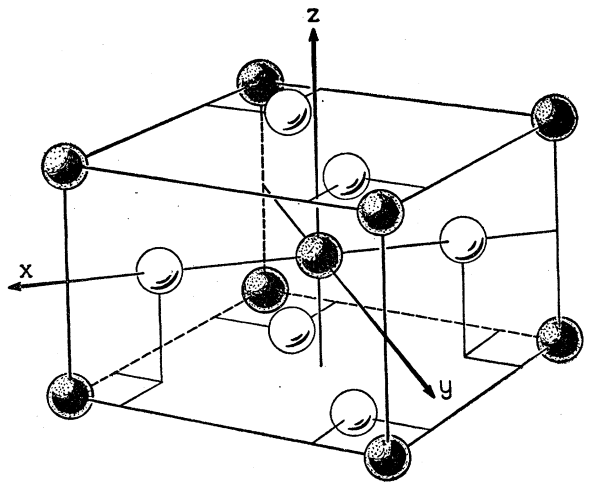

FIG. 1. Rutile type crystal structure of NiF_2. The solid and open circles represent Ni^{2+} and F^- ions, respectively.

to the $k=0$ wave of the lower frequency branch of the spin wave modes. The diminution of the length of the spins due to the crystalline field splitting is studied quantum-mechanically and some remarkable effects, which are expected when the crystalline field splitting is of comparable order of magnitude with or larger than the exchange energy, are discussed. In NiF_2 this effect seems to be small. Finally, possible structures of domains and domain-walls are studied based on the same model.

2. SPIN HAMILTONIAN

The rutile-type crystal structure of NiF_2 is shown in Fig. 1, together with the coordinate axes which we shall use below. There are two kinds of cation sites, the corner and the body center sites, in this crystal. The crystalline electric fields around these two sites have an orthorhombic symmetry and are the same except that their principal axes in the ab plane, i.e., the x and the y axes, are interchanged.

Ni^{2+} ion has a $(3d)^8$ configuration from which two triplet states ^3F and ^3P result. The energy of ^3P state is 14 000 cm^{-1} higher than ^3F for a free ion. When a Ni^{2+} ion is placed in a cubic crystalline field produced by an octahedron of anions around it, ^3F states split into one orbital singlet state Γ_2 and two orbital triplet states Γ_5 and Γ_4. The orbital singlet, Γ_2, state is the lowest and the separation between Γ_2 and Γ_5, the lowest excited state, is as big as 10^4 cm^{-1} (8500 cm^{-1} for Ni^{2+} surrounded by a water octahedron). In NiF_2 the orthorhombic component of the crystalline electric field lifts the degeneracy in the Γ_5, Γ_4, and $^3P(\Gamma_4)$ states. However, the splittings due to the orthorhombic component are considered to be smaller than that due to the cubic field, so that we may assume that the ground orbital state lies well below the first excited state, justifying a perturbation method which gives a spin Hamiltonian.

The spin Hamiltonian for NiF_2 may be written as follows:

$$\begin{aligned}\mathcal{H}=&J_1\sum_{\langle j,k\rangle 1}(\mathbf{S}_j\cdot\mathbf{S}_k)\\&+J_2\Big[\sum_{\langle j,j'\rangle 2}(\mathbf{S}_j\cdot\mathbf{S}_{j'})+\sum_{\langle k,k'\rangle 2}(S_k\cdot S_{k'})\Big]\\&+J_3\Big[\sum_{\langle j,j'\rangle 3}(\mathbf{S}_j\cdot\mathbf{S}_{j'})+\sum_{\langle k,k'\rangle 3}(\mathbf{S}_k\cdot\mathbf{S}_{k'})\Big]\\&+\sum_j\left[DS_{jz}^2-E(S_{jx}^2-S_{jy}^2)+\mu_B\mathbf{S}_j\cdot\mathbf{g}^{(1)}\cdot\mathbf{H}\right]\\&+\sum_k\left[DS_{kz}^2+E(S_{kx}^2-S_{ky}^2)+\mu_B\mathbf{S}_k\cdot\mathbf{g}^{(2)}\cdot\mathbf{H}\right],\end{aligned}\tag{2.1}$$

where j represents a corner site and k a body center site; $\langle\ \rangle 1$ under the summation sign means pairs of neighboring corner and body center cations, $\langle\ \rangle 2$ pairs of cations neighboring along the c axis, and $\langle\ \rangle 3$ those along the a or b axis, J_1, J_2, and J_3 denoting the corresponding exchange coupling constants; $\mathbf{g}^{(1)}$ and $\mathbf{g}^{(2)}$ are the g tensors of the cations at the corner and the body center sites, respectively, and $\mathbf{H}$ is the external magnetic field. The constants, D, E, $\mathbf{g}^{(1)}$, and $\mathbf{g}^{(2)}$, are given by a perturbation calculation as follows:

$$\begin{aligned}D&=\lambda^2(\Lambda_1+\Lambda_2-2\Lambda_z),\\E&=\lambda^2(\Lambda_1-\Lambda_2),\end{aligned}\tag{2.2}$$

$$\begin{aligned}g_x^{(1)}=g_y^{(2)}&=g_1=2(1-\lambda\Lambda_1),\\g_y^{(1)}=g_x^{(2)}&=g_2=2(1-\lambda\Lambda_2),\\g_z^{(1)}=g_z^{(2)}&=g_z=2(1-\lambda\Lambda_z),\end{aligned}\tag{2.3}$$

where

$$\begin{aligned}\Lambda_z&=\sum_n\frac{(g|L_z|n)(n|L_z|g)}{E_n-E_g},\\\Lambda_1&=\sum_n\frac{(g|L_x^{(1)}|n)(n|L_x^{(1)}|g)}{E_n-E_g},\\\Lambda_2&=\sum_n\frac{(g|L_y^{(1)}|n)(n|L_y^{(1)}|g)}{E_n-E_g},\end{aligned}\tag{2.4}$$

$\mathbf{L}^{(1)}$ denotes the orbital angular momentum of a cation at a corner site, λ the spin-orbit coupling constant whose numerical value for Ni^{2+} is -300 cm^{-1}, and g and n represent the ground and the excited states, respectively.

Here we neglected the dipole and pseudodipole interactions which, we think, are not of primary importance in this case.

3. PARAMAGNETIC SUSCEPTIBILITY

A calculation of the paramagnetic susceptibility of NiF_2 from the Hamiltonian (2.1) is rather straightforward[8] if we take a molecular field approximation for

[8] For example, Moriya, Motizaki, Kanamori, and Nagamiya, J. Phys. Soc. Japan **11**, 211 (1956).

the exchange interaction. The results are as follows:

$$\chi_{\parallel}=\chi_z=\frac{g_z^2\mu_B^2\delta_3}{E+(8J_1+2J_2+4J_3)\delta_3}+2\mu_B^2\Lambda_z,$$
$$\chi_{\perp}=\frac{(D+E)(g_1\mu_B)^2\delta_1+(D-E)(g_2\mu_B)^2\delta_2+2\mu_B^2[(g_1^2+g_2^2)(2J_2+4J_3)-2g_1g_2(8J_1)]\delta_1\delta_2}{D^2-E^2+2(2J_2+4J_3)[(D+E)\delta_1+(D-E)\delta_2]-4[(8J_1)^2-(2J_2+4J_3)^2]\delta_1\delta_2}+\mu_B^2(\Lambda_1+\Lambda_2), \tag{3.1}$$

where

$$\delta_1=\frac{1-e^{-(D-E)/kT}}{1+e^{-(D-E)/kT}+e^{-(D+E)/kT}},$$
$$\delta_2=\frac{1-e^{-(D+E)/kT}}{1+e^{-(D-E)/kT}+e^{-(D+E)/kT}}, \tag{3.2}$$
$$\delta_3=\frac{e^{-(D-E)/kT}-e^{-(D+E)/kT}}{1+e^{-(D-E)/kT}+e^{-(D+E)/kT}}.$$

At high temperatures, these expressions for the susceptibility components are well approximated by a Curie-Weiss law with additional terms of the temperature independent susceptibility. After some calculation we get at high temperatures

$$\chi_{\parallel}=\frac{2g_z^2\mu_B^2}{3k(T+\Theta_{\parallel})}+2\mu_B^2\Lambda_z,$$
$$\chi_{\perp}=\frac{(g_1^2+g_2^2)\mu_B^2}{3k(T+\Theta_{\perp})}+\mu_B^2(\Lambda_1+\Lambda_2), \tag{3.3}$$

where

$$\Theta_{\parallel}=[2(8J_1+2J_2+4J_3)+D]/3k,$$
$$\Theta_{\perp}=\left[2\left(\frac{2g_1g_2}{g_1^2+g_2^2}8J_1+2J_2+4J_3\right)-\tfrac{1}{2}D-\tfrac{3}{2}E\frac{g_1^2-g_2^2}{g_1^2+g_2^2}\right]\Big/3k. \tag{3.4}$$

According to the measurement by Matarrese and Stout,[2] $\chi_{\perp}$ is larger than $\chi_{\parallel}$ above the Néel temperature. We shall show that this means that D is positive. At high temperatures, we get from (3.3)

$$\chi_{\perp}-\chi_{\parallel}=\frac{(g_1^2+g_2^2-2g_z^2)\mu_B^2}{3k(T+\Theta)}+\frac{(g_1^2+g_2^2+2g_z^2)\mu_B^2}{3k(T+\Theta)^2}\Delta\Theta+\mu_B^2(\Lambda_1+\Lambda_2-2\Lambda_z), \tag{3.5}$$

where

$$\Theta=\tfrac{1}{2}(\Theta_{\parallel}+\Theta_{\perp}),$$
$$\Delta\Theta=\tfrac{1}{2}(\Theta_{\parallel}-\Theta_{\perp}). \tag{3.6}$$

With the use of (2.2) and (2.3), (3.5) is reduced to

$$\chi_{\perp}-\chi_{\parallel}=\left[\frac{8\mu_B^2}{3k|\lambda|(T+\Theta)}+\frac{3(g_1^2+g_2^2+2g_z^2)\mu_B^2}{4[3k(T+\Theta)]^2}+\frac{\mu_B^2}{\lambda^2}\right]D+\frac{4[1+2g_z^2/(g_1^2+g_2^2)]\mu_B^2}{[3k(T+\Theta)]^2}\left(\frac{8J_1}{|\lambda|}+\frac{3}{2}\right)\frac{E^2}{|\lambda|}. \tag{3.7}$$

D and E may be of the same order of magnitude and are much smaller than $|\lambda|$, and $8J_1$ is smaller than $|\lambda|$, so that the second term in the above expression (3.7) is regarded to be much smaller than the first term; we may safely neglect the second term. Then we can conclude that D is positive because its coefficient is definitely positive and the experimental values of $\chi_{\perp}-\chi_{\parallel}$ above the Néel temperature are positive. This conclusion is very important in determining the spin orientation below the Néel temperature as is shown in the following section.

We shall remark here that precise measurements of the susceptibility components $\chi_{\parallel}$ and $\chi_{\perp}$ above the Néel temperature as a function of temperature will make it possible to obtain the values of the parameters in the spin Hamiltonian (2.1).

4. SPIN ORDERING BELOW THE NÉEL TEMPERATURE

We shall take a two-sublattice model in which a magnetic unit cell is the same as a chemical unit cell. This assumption seems to be reasonable from the neutron diffraction data[4] as well as from the fact that the ratio of the paramagnetic Curie temperature ($\Theta_p\simeq 100\sim 116°K$)[9] to the Néel temperature ($T_N=73.2°K$) is nearly equal to those of MnF_2 and FeF_2, in which the spin orderings below the Néel temperatures are well established.[10]

[9] H. Bizette, J. phys. radium **12**, 161 (1951); DeHaas, Schultz, and Koolhaas, Physica **7**, 57 (1940).

[10] Recently Yoshimori [J. Phys. Soc. Japan **14**, 807 (1959)] showed that when $J_2/J_1>1$, a screw type spin-arrangement is stable. In this screw type structure, he obtained the following relation:

$$\frac{\Theta_p}{T_N}=\frac{4+(J_2/J_1)+2(J_3/J_1)}{2(J_2/J_1)^{-1}+(J_2/J_1)-2(J_3/J_1)}.$$

From a consideration of the superexchange interaction [P. W. Anderson, Phys. Rev. **115**, 2 (1959)] in NiF_2, J_1, J_2, and J_3 are considered to be all positive and the ratio (J_2/J_1) may not be so large. We may say, therefore, if the screw type structure of the spins is actually the case in NiF_2, Θ_p/T_N should be much larger than 1 in contrast to the observation. An example of the screw type structure is seen in MnO_2 where $\Theta_p/T_N\simeq 4$.

Now we shall adopt a molecular field approximation with classical spins. There are, of course, some quantum effects in nickel salts whose spin is 1. However, when the exchange interaction is sufficiently larger than the anisotropy energy, the classical spin model is considered to show all the essential characters. Even if the anisotropy is of considerable magnitude, we expect that at least qualitatively the classical spin model gives a correct answer to the problem. The possible quantum effects will be discussed in Sec. 8.

The length of a spin is written as S. The direction cosines of the corner and the body center spins are written as $(\alpha_1,\beta_1,\gamma_1)$ and $(\alpha_2,\beta_2,\gamma_2)$, respectively. The exchange and the anisotropy energies are expressed as follows:

$$\begin{aligned} E_{\rm ex}&=(N/2)8J_1S^2(\alpha_1\alpha_2+\beta_1\beta_2+\gamma_1\gamma_2),\\ E_{\rm an}&=(N/2)S^2[D(\gamma_1^2+\gamma_2^2)\\ &\qquad -E(\alpha_1^2-\beta_1^2-\alpha_2^2+\beta_2^2)]. \end{aligned} \tag{4.1}$$

From the symmetry of the crystal and the antiferromagnetic exchange coupling we may require the following conditions:

$$\gamma=-\gamma_2,\quad \alpha_1=-\beta_2,\quad \beta_1=-\alpha_2. \tag{4.2}$$

The total energy is then written as

$$\begin{aligned} E=(N/2)8J_1S^2\epsilon=&-(N/2)8J_1S^2[2\alpha_1\beta_1+\gamma_1^2\\ &-A_1\gamma_1^2+A_2(\alpha_1^2-\beta_1^2)], \end{aligned} \tag{4.3}$$

where

$$A_1=2D/8J_1,\quad A_2=2E/8J_1. \tag{4.4}$$

By a transformation,

$$\begin{aligned} \alpha_1&=\alpha_0\cos\theta-\beta_0\sin\theta,\\ \beta_1&=\alpha_0\sin\theta+\beta_0\cos\theta,\\ \gamma_1&=\gamma_0, \end{aligned} \tag{4.5}$$

where

$$\tan2\theta=1/A_2, \tag{4.6}$$

we get

$$\epsilon=-(1-A_1)\gamma_0^2-(1+A_2^2)^{\frac{1}{2}}(\alpha_0^2-\beta_0^2). \tag{4.7}$$

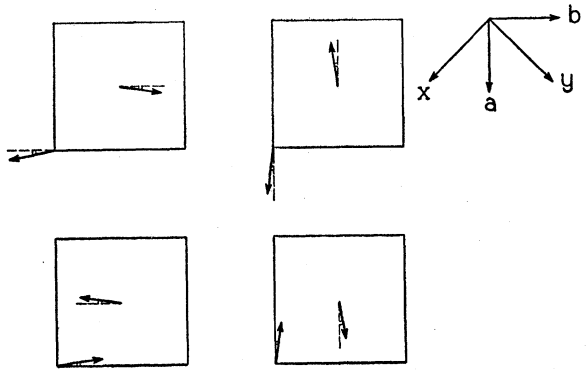

FIG. 2. Four equivalent arrangements of the spins in NiF_2 below the Néel temperature. The spins are lying in the ab plane.

We see from this expression that the following two types of spin orderings are possible.[11]

(1) When the condition,

$$(1-A_1)>(1+A_2^2)^{\frac{1}{2}} \tag{4.8}$$

is satisfied, the stable state is expressed by

$$\gamma_0=\gamma_1=-\gamma_2=1,\quad \alpha_0=\beta_0=0.$$

The spins are aligned along the $\pm c$ axes as in the case of MnF_2. The condition (4.8) is not satisfied in NiF_2, because D (and accordingly A_1) is positive as was seen in Sec. 3. There is no ferromagnetic moment in this case.

(2) When the condition,

$$(1-A_1)<(1+A_2^2)^{\frac{1}{2}} \tag{4.9}$$

is satisfied, the stable state is expressed by

$$\alpha_0=1,\quad \beta_0=\gamma_0=0,$$

or

$$\begin{aligned} \alpha_1=-\beta_2=\cos\theta&=\frac{1}{\sqrt{2}}\left(1+\frac{A_2}{(1+A_2^2)^{\frac{1}{2}}}\right)^{\frac{1}{2}},\\ \beta_1=-\alpha_2=\sin\theta&=\frac{1}{\sqrt{2}}\left(1-\frac{A_2}{(1+A_2^2)^{\frac{1}{2}}}\right)^{\frac{1}{2}}, \end{aligned} \tag{4.10}$$

$$\gamma_1=\gamma_2=0.$$

The spins are all perpendicular to the c axis, and the spins on the different sublattices are not exactly antiparallel; there is a net magnetic moment along the direction bisecting the x and y axes, i.e., along the a or b axis. This spin arrangement is shown in Fig. 2. The magnitude of the ferromagnetic moment is a function of $A_2=2E/8J_1$, and is given by

$$M=NS\mu_B(1/\sqrt{2})(g_1\cos\theta-g_2\sin\theta). \tag{4.11}$$

When $A_2\ll1$, or $|E|\ll8J_1$, we get

$$\begin{aligned} M&=NS\mu_B[\tfrac{1}{2}(g_1-g_2)+\tfrac{1}{4}(g_1+g_2)A_2]\\ &=NS\mu_B\left(\frac{g_1+g_2}{4}-\frac{8J_1}{2|\lambda|}\right)A_2. \end{aligned} \tag{4.12}$$

This second case is considered to be realized actually in NiF_2 since the condition (4.9) is satisfied because of the positive sign of D.

According to a torque measurement by Matarrese and Stout,[2] the easy direction of the ferromagnetic moment is the $\langle100\rangle$ direction in agreement with our present model. The magnitude of the ferromagnetic moment is simply proportional to A_2S as is seen in (4.12). From the

[11] Dzialoshinski[6] has shown the possible arrangements of spins in rutile-type crystals from a symmetry consideration. According to him there are five possible arrangements. However in our particular case of NiF_2, there are only two possibilities (1) and (2) corresponding to his I and II_1, because the spin value one of Ni^{2+} may not allow any anisotropy energy which is expressed in more than fourth power of the direction cosines; the coefficients f and g in his energy expression vanish.

numerical values: $\lambda=-300$ cm^{-1} and $8J_1=\frac{3}{4}k(T_N+\Theta_p)$ $\simeq 95$ cm^{-1}, we may assume

$$\left(\frac{g_1+g_2}{4}-\frac{8J_1}{2|\lambda|}\right)\simeq 1.$$

An analysis of the torque curves, which will be described in the following section, gives

$$|A_2|S=M/N\mu_B\simeq 0.03,$$

so that

$$M=170 \text{ erg gauss}^{-1} \text{ mole}^{-1}. \tag{4.13}$$

5. SPIN ORIENTATION UNDER THE MAGNETIC FIELD—TORQUE

In this section we shall study the equilibrium orientation of the spins under the magnetic field and make a comparison between the theoretical and experimental torque curves. We shall here describe only the physics and leave the detailed calculations to Appendix I.

Let us first consider the effective anisotropy energy of the ferromagnetic moment and the magnitude of the moment as a function of its direction. The change of the magnitude of the ferromagnetic moment is caused by the change of the angle between $\mathbf{S}_1$ and $\mathbf{S}_2$. These are easily obtained by the following simple consideration: The spins $\mathbf{S}_1$ and $\mathbf{S}_2$ are in the ab plane and their directions are denoted by the angles φ_1 and φ_2 measured from the [100] direction. General definition of the polar angles of the spins and the magnetic field are shown in Fig. 3. When $H=0$, $\theta_1=\theta_2=\pi/2$. The exchange and the anisotropy energies are written as

$$\begin{aligned} E_{ex}&=\tfrac{1}{2}N8J_1S^2\cos(\varphi_2-\varphi_1),\\ E_{an}&=\tfrac{1}{2}NES^2(\sin 2\varphi_1-\sin 2\varphi_2). \end{aligned} \tag{5.1}$$

With the definitions:

$$\psi=(\varphi_2-\varphi_1)/2, \quad \varphi=(\varphi_1+\varphi_2)/2, \tag{5.2}$$

we write

$$E_{tot}=\tfrac{1}{2}N8J_1S^2(\cos 2\psi-A_2\cos 2\varphi\sin 2\psi). \tag{5.3}$$

Here φ means the direction of the net magnetic moment, and 2ψ the angle between $\mathbf{S}_1$ and $\mathbf{S}_2$. The value of ψ which makes E_{tot} given by (5.3) minimum with the fixed value of φ is given by

$$\tan 2\psi=-A_2\cos 2\varphi. \tag{5.4}$$

Therefore, the effective anisotropy energy and the ferromagnetic moment as a function of φ are written as follows:

$$\begin{aligned} E(\varphi)&=-4NJ_1S^2(1+A_2^2\cos^2 2\varphi)^{\frac{1}{2}}\\ &\simeq -4NJ_1S^2(1+\tfrac{1}{2}A_2^2\cos^2 2\varphi), \end{aligned} \tag{5.5}$$

$$\begin{aligned} M(\varphi)&=Ng\mu_BS\cos\psi\\ &\simeq \tfrac{1}{2}Ng\mu_BSA_2\cos 2\varphi. \end{aligned} \tag{5.6}$$

The effective ferromagnetic anisotropy energy has a cubic symmetry with the easy directions in the ⟨100⟩ directions and its magnitude is smaller than the anisotropy energy E of a single spin in the ab plane by a multiplicative factor A_2. The net magnetic moment depends strongly on its direction. It should be noted that as we go from $\varphi=0$ to $\varphi=\pi/2$, the moment becomes smaller; the moment vanishes at $\varphi=\pi/4$ and becomes negative at $\varphi>\pi/4$.

The external magnetic field gives two effects. One is to change the direction of the net magnetic moment and the other is to induce a magnetic moment just as in antiferromagnets. It is easily seen that when the magnetic field is much smaller than $E/g\mu_B$ [E is the anisotropy energy defined by (2.1)] the change of the direction of the net moment is very small. This is due to the small magnitude of the net magnetic moment and to its angular dependence given by (5.6). Because of the latter effect the direction of the net magnetic moment which gives a minimum magnetic energy is not parallel to the magnetic field but is inclined toward the closest ⟨100⟩ direction.

The torque in the limit of the weak magnetic field is given as follows: (1) Magnetic field in the (001) plane; torque along the c axis.

$$T_{[001]}/H\simeq M_0\sin\theta_0,$$

where θ_0 is the angle between the magnetic field and the [100] axis, and M_0 denotes the net magnetic moment under no magnetic field. (2) Magnetic field in the (110) plane; torque along the [110] direction.

$$T_{[110]}/H\simeq(1/\sqrt{2})M_0\sin\theta_0,$$

where θ_0 is the angle between the magnetic field and the [1$\bar{1}$0] direction. The ratio $T_{[001]}/T_{[110]}=\sqrt{2}$ and the angular dependences of the torques agree very well with the experiment.

The field dependent part of the torque is mainly due to the field induced part of the magnetic moment. The

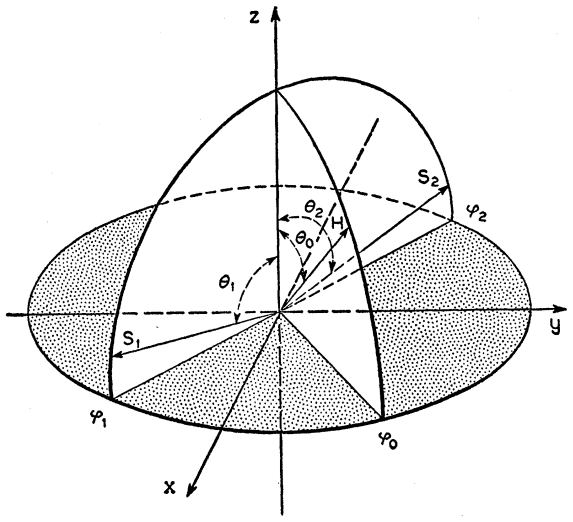

FIG. 3. Definition of the polar angles of $\mathbf{S}_1$, $\mathbf{S}_2$, and $\mathbf{H}$.

susceptibility components along the directions perpendicular to $\mathbf{S}_1-\mathbf{S}_2$, i.e., along the $\langle 100\rangle$ and [001] directions are essentially $\chi_\perp$ in antiferromagnets which is given by $\chi_\perp=Ng^2\mu_B{}^2/8J_1$ in the first approximation. Thus we see that the field dependent part of the torque shows a similar behavior as that in usual antiferromagnets. The reverse field dependences of the torques in the two cases measured by Matarrese and Stout [H in (001) plane and H in (110) plane] are clearly understood

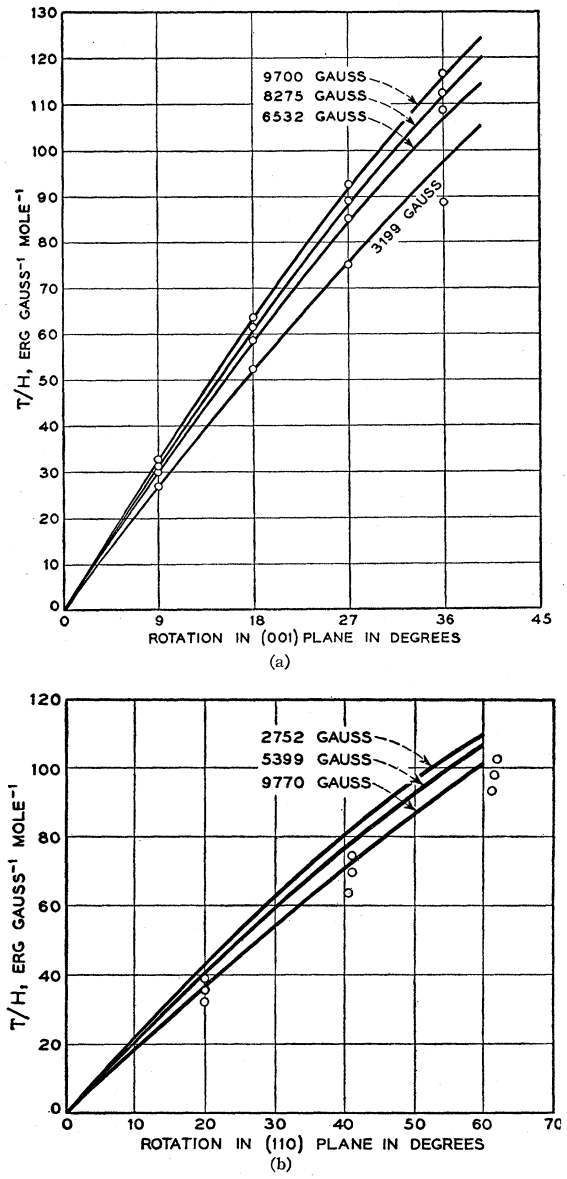

FIG 4. (a) Molal perpendicular magnetization, or torque divided by magnetic field, *versus* angle between field and [100] direction. Rotation in (001) plane. Theoretical values are shown by the solid lines and experimental points are shown by the cross marks. (b) Molal perpendicular magnetization, or torque divided by magnetic field, *versus* angle between field and [110] direction. Rotation in (110) plane. Theoretical values are shown by the solid lines and experimental points are shown by the cross marks.

from this point of view. A remarkable fact is that the field dependent part of the torque curves depends essentially on the direction of the spin ordering, i.e., the direction of $\mathbf{S}_1-\mathbf{S}_2$, and very little on the anisotropy energy provided the anisotropy energy is larger than the magnetic energy. We may say, therefore, that the field dependent part of the torque curves tells in what direction the spins are aligned. The field dependent part of the measured torque curves in the (001) and (110) planes are explained by taking the direction of $\mathbf{S}_1-\mathbf{S}_2$ along the [010] axis, consistent with our present model.

A comparison between the detailed calculation (given in Appendix I) and the experiment is shown in Fig. 4(a) and Fig. 4(b). The numerical values used in addition to those given in the preceding section are

$$(g_1+g_2)/4=1.2,\quad 8J_1/|\lambda|=0.3,\quad \text{and}\quad A_2S=0.03,\quad (5.7)$$

where A_2S was determined so as to get the best fit of the formula (A.12) with the measurement in the (001) plane. The agreement is excellent both qualitatively and quantitatively. The departure of the experimental points from the theoretical curve near 45° in the (001) plane may come from some secondary effects. At 45° there is no preference for the direction of the net magnetic moment between the [100] and [010] directions. Moments in some domains may point in one and those in the others point in the other direction; their effect will thus be cancelled, i.e., the torque at 45° may be zero. Near 45° there may be some distribution of domains between those pointing nearly in the [100] direction and those pointing nearly in the [010] direction.

We shall finally predict that in the {100} plane the field dependence of the torque is almost one order of magnitude smaller than in the (001) plane. This is expected because of the nearly isotropic susceptibility in the {100} plane.

6. NUCLEAR MAGNETIC RESONANCE OF FLUORINES

We shall briefly sketch the nuclear resonance frequencies of the fluorines expected from our present model. As the nuclear spins see the local field coming from the individual spins of Ni^{2+}, the spin arrangement below the Néel temperature can be studied by this method. From the consideration of the crystal structure including the Ni^{2+} spins below the Néel temperature, it is clear that there are two kinds of fluorine site in the absence of the external magnetic field. The local fields at these sites are perpendicular to the c axis and one of them is obtained by a 180° rotation of the other around the [100] direction in which the net ferromagnetic moment is directed.

As was discussed in Sec. 5, the spin directions are changed very little by the external magnetic field, unless the latter is too strong. The local field at the fluorines are, therefore, approximately the vector sum of the external field and the local field in the absence of the

external field. For example, if the magnetic field is applied along the c axis, the resonance frequency is given by

$$\omega=\gamma(H^2+H_{\rm loc}^2)^{\frac{1}{2}}, \tag{6.1}$$

where γ is the gyromagnetic ratio of F^{19} nuclei, and H, and $H_{\rm loc}$ are the external magnetic field and the local magnetic field in the absence of the external field, respectively.

According to Shulman's recent experiment,[5] this relation is actually satisfied. This also strongly supports our present theory. The detailed analysis of the nuclear resonance data will be reported by Shulman.

7. SPIN WAVES AND MAGNETIC RESONANCE FREQUENCIES

We shall study in this section the frequency spectra of the spin waves and the magnetic resonance frequencies by using a continuum model which is good for spin waves of long wavelengths. The procedure is an antiferromagnetic counterpart of the Herring-Kittel theory of ferromagnetic spin waves.[12] We need two variables corresponding to the two sublattice magnetizations. The spin densities corresponding to the two sublattices are defined by

$$\begin{aligned}\mathbf{S}_1(\mathbf{r})&=-(2/N)\textstyle\sum_j \delta(\mathbf{r}-\mathbf{r}_j)\mathbf{S}_j,\\ \mathbf{S}_2(\mathbf{r})&=-(2/N)\textstyle\sum_k \delta(\mathbf{r}-\mathbf{r}_k)\mathbf{S}_k.\end{aligned} \tag{7.1}$$

The negative signs are taken in order to make the spin densities parallel (not antiparallel) to the sublattice magnetizations. We shall assume, for simplicity, that g is isotropic and neglect the exchange interaction between the spins in the same sublattice. The Hamiltonian (2.1) is then rewritten as

$$\begin{aligned}\mathcal{H}=(N/2)8J_1\Big[&\int \mathbf{S}_1(\mathbf{r})\cdot\mathbf{S}_2(\mathbf{r})dv\\ &+A\int \mathbf{S}_1\cdot\Delta\mathbf{S}_2 dv+\tfrac{1}{2}A_1\int(S_{1z}^2+S_{2z}^2)dv\\ &-\tfrac{1}{2}A_2\int(S_{1x}^2-S_{1y}^2-S_{2x}^2+S_{2y}^2)dv\\ &-B\int\mathbf{h}\cdot(\mathbf{S}_1+\mathbf{S}_2)dv\Big],\end{aligned} \tag{7.2}$$

where

$$A=a^2/8,$$

a being a lattice constant along the a axis,

$$B=g\mu_B H/8J_1 S,$$

and

$$\mathbf{h}=\mathbf{H}/H.$$

A_1 and A_2 are defined by (4.4) and the scale of the z direction is changed by a factor (c/a). When the spin densities $\mathbf{S}_1(\mathbf{r})$ and $\mathbf{S}_2(\mathbf{r})$ are changed by arbitrary small amounts, the corresponding energy change is expressed by

$$\begin{aligned}\delta\mathcal{H}=(N/2)8J_1\int dv\,[&\delta\mathbf{S}_1\cdot(\mathbf{S}_2+A\Delta\mathbf{S}_2+A_1S_{1z}\mathbf{n}\\ &-A_2S_{1x}\mathbf{l}+A_2S_{1y}\mathbf{m}-BS\mathbf{h})+\delta\mathbf{S}_2\cdot(\mathbf{S}_1+A\Delta\mathbf{S}_1\\ &+A_1S_{2z}\mathbf{n}+A_2S_{2x}\mathbf{l}-A_2S_{2y}\mathbf{m}-BS\mathbf{h})],\end{aligned} \tag{7.3}$$

where $\mathbf{l}$, $\mathbf{m}$, and $\mathbf{n}$ are unit vectors pointing in the x, y, and z directions, respectively. The effective magnetic fields for the two kinds of spins are

$$\begin{aligned}\mathbf{H}_{\rm eff}^{(1)}&=(8J_1/g\mu_B)[\mathbf{S}_2+A\Delta\mathbf{S}_2+A_1S_{1z}\mathbf{n}\\ &\qquad -A_2S_{1x}\mathbf{l}+A_2S_{1y}\mathbf{m}-BS\mathbf{h}],\\ \mathbf{H}_{\rm eff}^{(2)}&=(8J_1/g\mu_B)[\mathbf{S}_1+A\Delta\mathbf{S}_1+A_1S_{2z}\mathbf{n}\\ &\qquad +A_2S_{2x}\mathbf{l}-A_2S_{2y}\mathbf{m}-BS\mathbf{h}].\end{aligned} \tag{7.4}$$

The equations of motion are given by

$$\hbar(d/dt)\mathbf{S}_1=-g\mu_B\mathbf{S}_1\times\mathbf{H}_{\rm eff}^{(1)}, \tag{7.5a}$$

$$\hbar(d/dt)\mathbf{S}_2=-g\mu_B\mathbf{S}_2\times\mathbf{H}_{\rm eff}^{(2)}. \tag{7.5b}$$

As we are looking for the modes of small vibrations of the spins near the equilibrium position, it is advantageous to choose the equilibrium direction of the spin as one of the three coordinate axes. We shall introduce two coordinate systems (ξ,η,ζ) and (ξ',η',ζ') as shown in Fig. 5. The ζ and ζ' axes will be chosen to be along the equilibrium directions of $\mathbf{S}_1$ and $\mathbf{S}_2$, respectively. The unit vectors along the ξ, η, ζ, ξ', η', and ζ' axes are written as $\mathbf{l}_1$, $\mathbf{m}_1$, $\mathbf{n}_1$, $\mathbf{l}_2$, $\mathbf{m}_2$, and $\mathbf{n}_2$, respectively. The polar angles of these axes referring to the original

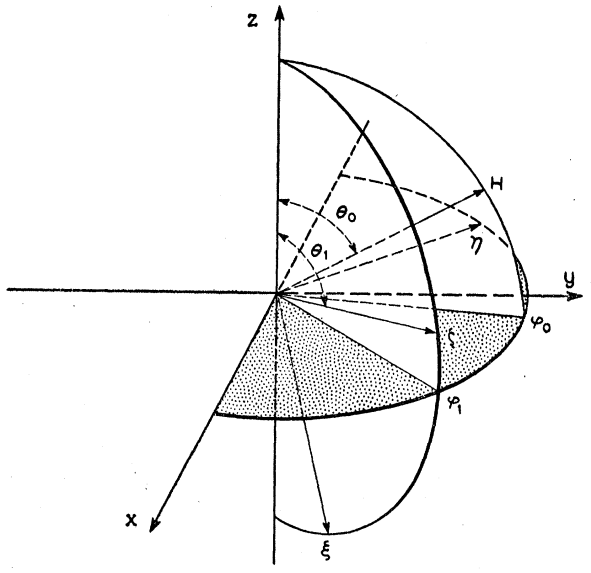

FIG. 5. Orientation of ξ, η, and ζ coordinate axes. ξ', η', and ζ' axes are defined by replacing θ_1 and φ_1 in the (ξ,η,ζ) system with θ_2 and φ_2.

[12] C. Herring and C. Kittel, Phys. Rev. **81**, 869 (1951).

coordinate system are given in the following equations:

$$\begin{aligned}\mathbf{l}&=\mathbf{l}_i\cos\theta_i\cos\varphi_i-\mathbf{m}_i\sin\varphi_i+\mathbf{n}_i\sin\theta_i\cos\varphi_i,\\ \mathbf{m}&=\mathbf{l}_i\cos\theta_i\sin\varphi_i+\mathbf{m}_i\cos\varphi_i+\mathbf{n}_i\sin\theta_i\sin\varphi_i,\\ \mathbf{n}&=-\mathbf{l}_i\sin\theta_i+\mathbf{n}_i\cos\theta_i.\end{aligned}\tag{7.6}$$

The polar angles of the magnetic field are written as θ_0, φ_0.

Now we shall express the equations of motion (7.5) in the new coordinate systems; the components of $\mathbf{S}_1$ are written in the (ξ,η,ζ) system and those of $\mathbf{S}_2$ in the (ξ',η',ζ') system. Linearization of the equations of motion is carried out simply by neglecting the terms more than quadratic with respect to $S_{1\xi}$, $S_{1\eta}$, $S_{2\xi'}$, and $S_{2\eta'}$. Two out of the six equations, the ζ component of (7.5a) and the ζ' component of (7.5b), give the equilibrium conditions of the spins; they are shown in Appendix II. These equilibrium conditions are the same as those treated in the preceding sections. The other four components represent the spin wave motion. They are

$$\begin{aligned}(1/\omega_e)\dot{S}_{1\xi}&=aS_{1\xi}+(c+d)S_{1\eta}+pS_{2\xi'}+qS_{2\eta'},\\ (1/\omega_e)\dot{S}_{1\eta}&=-(c-d)S_{1\xi}-aS_{1\eta}+rS_{2\xi'}+sS_{2\eta'},\end{aligned}\tag{7.7}$$

$$\begin{aligned}(1/\omega_e)\dot{S}_{2\xi'}&=-sS_{1\xi}+qS_{1\eta}-bS_{2\xi'}+(e+f)S_{2\eta'},\\ (1/\omega_e)\dot{S}_{2\eta'}&=rS_{1\xi}-pS_{1\eta}-(e-f)S_{2\xi'}+bS_{2\eta'},\end{aligned}\tag{7.8}$$

where $\omega_e=8J_1S/\hbar$. General expressions for the coefficients in (7.7) are given in Appendix III. They can be evaluated in general and when the external field is not strong, i.e., B/A_2 and B/A_1 are sufficiently smaller than 1, the expressions in (A.10) are applicable together with (A.2) and (A.5).

We shall give here some simple examples: the spin wave frequency spectra without the influence of the magnetic field and the magnetic resonance frequencies due to a uniform oscillating field under a constant magnetic field in the *ab* plane. The other cases are easily calculated in the same way.

(1) *Spin Wave Frequency Spectra* ($H=0$)

When the external field is absent, the coefficients in (7.7) are simply as follows:

$$\begin{aligned}&a=b=p=s=0,\\ &c=e=1+\tfrac{1}{2}A_1+A_2^2,\\ &d=f=-\tfrac{1}{2}A_1+\tfrac{1}{2}A_2^2,\\ &q=-(1-Ak^2)(1-\tfrac{1}{2}A_2^2),\\ &r=-(1-Ak^2),\end{aligned}\tag{7.9}$$

where k is a wave number of a spin wave. The secular equation is then written

$$(\omega/\omega_e)^4-2B(\omega/\omega_e)^2+C=0,\tag{7.10}$$

with

$$\begin{aligned}B&=c^2-d^2-(1-\tfrac{1}{2}A_2^2)(1-Ak^2)^2,\\ C&=B^2-[c+d-(c-d)(1-\tfrac{1}{2}A_2^2)]^2(1-Ak^2)^2.\end{aligned}\tag{7.11}$$

Thus we get the following two branches of the frequency spectra:

$$\begin{aligned}\omega_1&=\omega_e[2A_1+(2-A_1)Ak^2]^{\frac{1}{2}},\\ \omega_2&=\omega_e[(2A_2)^2+(2+A_1)Ak^2]^{\frac{1}{2}}.\end{aligned}\tag{7.12}$$

These dispersion relations are similar in form to that of antiferromagnetic spin waves under the presence of an anisotropy. Actually, the first branch, ω_1, has just the same form as in usual antiferromagnets. However the second one, ω_2, has a different character, that is, the lowest frequency ($k=0$) corresponds to the anisotropy energy instead of an average of the exchange and anisotropy energy as in the case of usual antiferromagnets. This means that there are spin wave modes of much lower frequencies in NiF_2 than in the other iron group difluorides, MnF_2, FeF_2, and CoF_2. According to the specific heat measurement and its analysis by Stout and Catalano,[3] the spin contribution to the specific heat at low temperatures of NiF_2 is larger than that of FeF_2 and its temperature dependence is weaker than that of any other iron group difluorides. This seems to agree qualitatively, though not quantitatively, with the nature of the spin wave frequency spectra obtained here.

(2) *Magnetic Resonance Frequencies* (*H in the ab Plane*)

Magnetic resonance frequencies due to the uniform oscillating field will be obtained by putting $k=0$ in (7.7). For simplicity, we shall treat the case where a magnetic field is applied in the *ab* plane, i.e., $\theta_0=\pi/2$. The coefficients in (7.7) are given by

$$\begin{aligned}&a=b=p=s=0,\\ &c=1+\tfrac{1}{2}A_1+A_2^2-\tfrac{1}{4}B\sin\psi_0+A_2B\cos\psi_0,\\ &d=-\tfrac{1}{2}A_1+\tfrac{1}{2}A_2^2+\tfrac{1}{4}B\sin\psi_0+\tfrac{1}{2}A_2B\cos\psi_0,\\ &e=1+\tfrac{1}{2}A_1+A_2^2+\tfrac{1}{4}B\sin\psi_0+A_2B\cos\psi_0,\\ &f=-\tfrac{1}{2}A_1+\tfrac{1}{2}A_2^2-\tfrac{1}{4}B\sin\psi_0+\tfrac{1}{2}A_2B\cos\psi_0,\\ &q=-(1-\tfrac{1}{2}A_2^2),\\ &r=-1.\end{aligned}\tag{7.13}$$

The same type of secular equation as in (1) leads to the following resonance frequencies:

$$\begin{aligned}\omega_1&=\omega_e[2A_1+A_2^2+A_2B\cos\psi_0]^{\frac{1}{2}},\\ \omega_2&=\omega_e[(2A_2)^2+5A_2B\cos\psi_0]^{\frac{1}{2}},\end{aligned}\tag{7.14}$$

where ψ_0 is the angle between the (100) direction, in which the net moment is directed, and the direction of the magnetic field; $|\psi_0|$ should be smaller than $\pi/4$. The lowest resonance frequency is

$$\omega=2A_2\omega_e=4ES/\hbar,$$

whose numerical value is estimated to be

$$(\omega/2\pi)=8J_12A_2S/h\cong1.7\times10^{11},$$

corresponding to a wavelength of about 2 mm.

8. DIMINUTION OF THE LENGTH OF SPIN

The treatment given so far is classical except the calculation of the paramagnetic susceptibility. We believe that the classical treatment gives, at least qualitatively, a correct answer to this problem of NiF_2. However, it is needed to study what kind of effect is expected from a quantum mechanical treatment and how large the effect is.

When the crystalline electric field has an orthorhombic symmetry, the spin states split into three singlets even without the magnetic field or the exchange interaction[13]; there is no Kramers degeneracy. Each state has no magnetic moment associated with it. The external magnetic field as well as the exchange interaction gives rise to a polarization of each state. When the exchange interaction is sufficiently larger than the crystalline field splitting of the spin levels, the expectation value of a spin at 0°K will be nearly equal to one. On the other hand, when the spin level splitting is of comparable order of magnitude with the exchange interaction, the expectation value of a spin at 0°K will be appreciably diminished. As we shall see later in this section, when the splitting between the lowest two spin levels is more than two times larger than the exchange energy, there is no antiferromagnetic state at all, at least within the framework of a molecular field theory.

To simplify the problem, we shall consider the case of an orthorhombic crystal in which all the cation sites have the same crystalline field. Taking a two sublattice model with the nearest neighbor interactions, we may write the spin Hamiltonian for the spins on the two sublattices as follows:

$$\begin{aligned}\mathcal{H}^{(1)}&=DS_{1z}^2-E(S_{1x}^2-S_{1y}^2)+JzS_{1x}\langle S_{2x}\rangle,\\ \mathcal{H}^{(2)}&=DS_{2z}^2-E(S_{2x}^2-S_{2y}^2)+JzS_{2x}\langle S_{1x}\rangle,\end{aligned}\tag{8.1}$$

where again a molecular field approximation was adopted in expressing the exchange interaction, J is the exchange coupling constant between the neighboring spins, z is the number of nearest neighbors, and D and E are taken positive without loss of generality. The easy direction of the spins is then assumed to be along the x axis. With the abbreviation:

$$Jz\langle S_{2x}\rangle=h_1,\quad Jz\langle S_{1x}\rangle=h_2,\tag{8.2}$$

we have the following matrix for the Hamiltonian:

$$\mathcal{H}^{(i)}=\begin{bmatrix}-\frac{1}{2}(D+3E)+h_i & 0 & \frac{1}{2}(D-E)\\ 0 & 0 & 0\\ \frac{1}{2}(D-E) & 0 & -\frac{1}{2}(D+3E)-h_i\end{bmatrix},\tag{8.3}$$

where $i=1, 2$. This is diagonalized by a transformation:

$$\bar{U}_i=\begin{bmatrix}\cos\theta_i & 0 & \sin\theta_i\\ 0 & 1 & 0\\ -\sin\theta_i & 0 & \cos\theta_i\end{bmatrix},\tag{8.4}$$

with

$$\tan 2\theta_i=(D-E)/2h_i.\tag{8.5}$$

We get the following energy eigenvalues:

$$\begin{aligned}E_1^{(i)}&=-\tfrac{1}{2}(D+3E)+[\tfrac{1}{4}(D-E)^2+h_i^2]^{\frac{1}{2}},\\ E_2^{(i)}&=0,\\ E_3^{(i)}&=-\tfrac{1}{2}(D+3E)-[\tfrac{1}{4}(D-E)^2+h_i^2]^{\frac{1}{2}}.\end{aligned}\tag{8.6}$$

The statistical average of a spin is given by

$$\begin{aligned}\langle S_{iz}\rangle&=\sum_n\frac{\partial E_n^{(i)}}{\partial h_i}\exp[-E_n^{(i)}/kT]/\sum_n\exp[-E_n^{(i)}/kT]\\ &=-\frac{h_i}{[\frac{1}{4}(D-E)^2+h_i^2]^{\frac{1}{2}}}2\sinh\{[\tfrac{1}{4}(D-E)^2+h_i^2]^{\frac{1}{2}}/kT\}\\ &\quad\times(e^{-(D+3E)/2kT}\\ &\qquad+2\cosh\{[\tfrac{1}{4}(D-E)^2+h_i^2]^{\frac{1}{2}}/kT\})^{-1}.\end{aligned}\tag{8.7}$$

This equation should be solved for

$$\langle S_x\rangle=\langle S_{1x}\rangle=-\langle S_{2x}\rangle.$$

With the abbreviation

$$\begin{aligned}x&=[\langle S_x\rangle^2+((D-E)/2Jz)^2]^{\frac{1}{2}},\\ \theta&=kT/Jz,\\ d&=(D+3E)/2Jz,\end{aligned}\tag{8.8}$$

we get

$$x=\frac{2\sinh(x/\theta)}{e^{-d/\theta}+2\cosh(x/\theta)}.\tag{8.9}$$

At the absolute zero temperature, this becomes simply

$$x=\{\langle S_x\rangle^2+[(D-E)/2Jz]^2\}^{\frac{1}{2}}=1,$$

or

$$\langle S_x\rangle=\{1-[(D-E)/2Jz]^2\}^{\frac{1}{2}}.\tag{8.10}$$

This shows the diminution of the expectation value of a spin due to the crystalline electric field.

In order to have a nonimaginary value of $\langle S_x\rangle$ in (8.10), $(D-E)/2$ must be smaller than Jz. This requirement is just the same as the condition for the existence of an antiferromagnetic state, or a Néel temperature, as we shall show below.

The Néel temperature is obtained by putting $\langle S_{iz}\rangle\to 0$ in (8.7). With the abbreviation

$$\begin{aligned}&2D/Jz=A_1,\quad 2E/Jz=A_2,\\ &kT_N/Jz=\theta_N,\end{aligned}\tag{8.11}$$

we get

$$\begin{aligned}&e^{-(A_1+3A_2)/4\theta_N}+2\cosh[(A_1-A_2)/4\theta_N]\\ &\quad=[8/(A_1-A_2)]\sinh[(A_1-A_2)/4\theta_N].\end{aligned}\tag{8.12}$$

From this equation we can see that the condition for the existence of a Néel temperature is

$$\tfrac{1}{4}|A_1-A_2|<1,$$

[13] When the crystal symmetry is tetragonal and the axis is the hard direction for the spins ($D>0$, $E=0$), the lowest energy state is singlet. The succeeding argument is valid for this case, too.

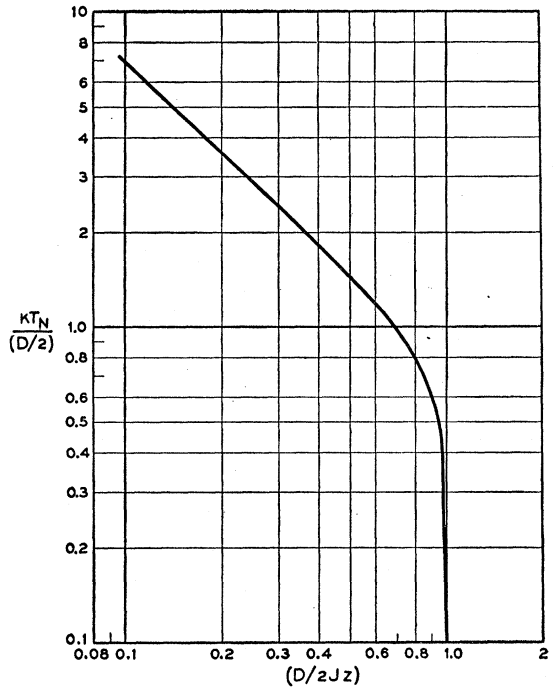

FIG. 6. Néel temperature of tetragonal nickel salts, whose tetragonal axis is the hard direction of the spins, *versus* ratio of anisotropy energy to exchange energy.

or

$$\tfrac{1}{2}|D-E|<Jz, \tag{8.13}$$

in consistence with the condition for $\langle S_x\rangle$ in (8.10) to have a real value.

The absence of the antiferromagnetism discussed above may be expected in some magnetically dilute salts. We may see a very rapid decrease of the Néel temperature when we dilute samples gradually. Numerical values of $\theta_N=kT_N/(D/2)$ as a function of $a=D/2Jz$ are shown in Fig. 6, where E is taken to be zero. The effect of D on the Néel temperature is small except where $a=D/2Jz$ is larger than about 0.8.

In the case of NiF_2, the argument given above is not strictly applicable because of the two kinds of sites in a unit cell. Though it is possible to extend the same type of calculation to NiF_2, we shall here simply contend ourselves with the following approximate consideration. As we have seen in the classical treatment, the spins in NiF_2 are almost aligned along one line and the deviation from it is very small owing to the small value of E/Jz. So we may approximately evaluate the value of $\langle S\rangle$ by taking $E\simeq 0$. Then we have

$$\langle S\rangle\simeq[1-(D/2Jz)^2]^{\frac{1}{2}}.$$

From the measured anisotropy of the susceptibility the value of D may roughly be estimated from (3.7). We get $D\sim 6$ cm^{-1} from the value of $\chi_\perp-\chi_{11}=1.102\times10^{-4}$ at 301.15°K.[2] This value is rather big as compared with those measured in other nickel salts. $\langle S\rangle$ is very close to 1.

9. DOMAINS AND DOMAIN WALLS

As we have seen in Sec. 4, there are four equivalent arrangements of the spins in which the net magnetic moments are pointing in the ⟨100⟩ directions. When the magnetic field is absent, the crystal is naturally divided into domains of these four kinds of magnetization direction. We shall briefly discuss a possible structure of domains and domain-walls.

The high anisotropy energy in the [001] direction makes a domain wall perpendicular to the *ab* plane highly unfavorable. On the other hand, the effective ferromagnetic anisotropy energy in the *ab* plane is more than two orders of magnitude smaller than that out of the *ab* plane. We may expect, therefore, that a domain wall perpendicular to the *c* axis is energetically the most favorable one. A favorable domain shape then is a flat plate perpendicular to the *c* axis. We shall further discuss on this type of domains and domain walls.

The spin arrangement in a domain wall is deduced from Fig. 2 and from the discussion in Sec. 5, particularly from (5.6). The expected arrangements of the ferromagnetic moments in a 90° wall and a 180° wall are shown in Fig. 7(a) and Fig. 7(b), respectively. The sublattice spins are rotating gradually as we proceed along the *c* axis, and at the same time the angle between the two sublattices are changing. The ferromagnetic moment at the middle of a 90° wall is zero. The directions of the two sublattices in both sides of the domain-walls are shown in the same figures.

Now we shall estimate the wall energy and thickness. When a 90° wall consists of n atomic layers perpendicular to the *c* axis, the anisotropy energy per unit area may be given by

$$\sigma_{\rm an}\simeq EA_2S^2n/a^2, \tag{9.1}$$

where a is a lattice constant. While the exchange energy is estimated as

$$\sigma_{\rm ex}\simeq(nJzS^2/2a^2)(\pi/2n)^2. \tag{9.2}$$

n is determined so as to make $\sigma_{\rm wall}=\sigma_{\rm an}+\sigma_{\rm ex}$ minimum. We get

$$n\simeq\pi Jz/4E\sim 40. \tag{9.3}$$

This value is one order of magnitude smaller than in the case of iron. A more precise calculation leads essentially to the same result. The wall energy is given by

$$\sigma_{\rm wall}\simeq ES^2/a^2\sim 0.1\ \text{erg}, \tag{9.4}$$

which is one order of magnitude smaller than that in iron. The wall thickness and energy of a 180° wall may be twice as large as those of a 90° wall.

Let us now estimate the size of a domain in a crystal with rectangular cross sections as shown in Fig. 8. We shall consider a domain structure shown in Fig. 8. The magnetostatic energy per unit area in the *bc* plane is

given by[14]

$$w_{\text{mag}}=1.7I_s^2d, \tag{9.5}$$

where I_s is the magnetization per unit volume, d the domain width in the c direction. The wall energy per unit area in the bc plane is given by

$$w_{\text{wall}}\simeq 2ES^2l/a^2d. \tag{9.6}$$

The total energy per unit area is

$$w=w_{\text{mag}}+w_{\text{wall}},$$

which is a minimum with respect to the domain width d when

$$d=(2ES^2l/1.7I_s^2a^2)^{\frac{1}{3}}. \tag{9.7}$$

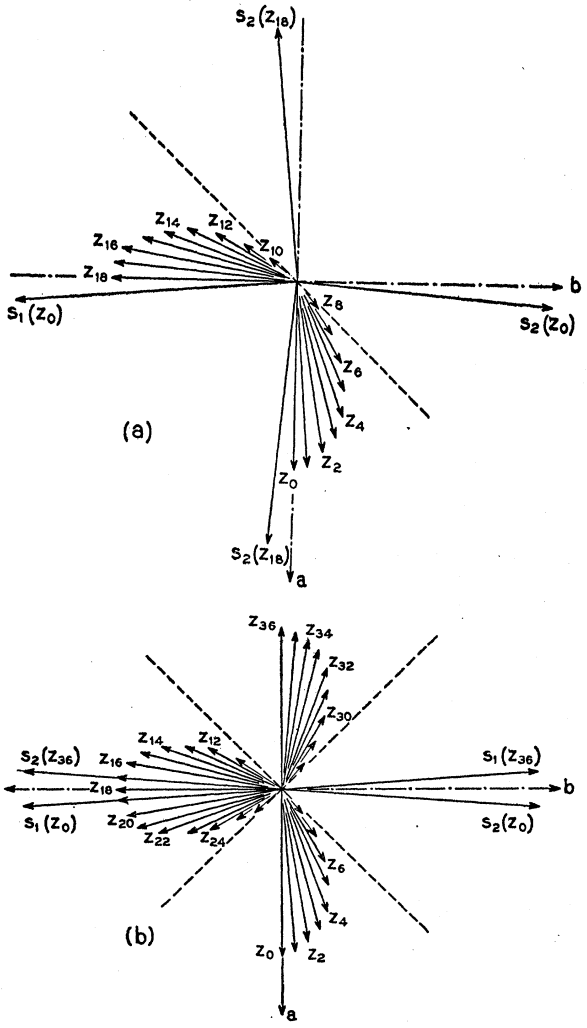

FIG. 7. (a) Rotation of magnetization in a 90° domain wall in NiF_2. The moments are in the ab plane and z_i indicates z coordinate which becomes larger as i increases. Directions of sublattice magnetizations in the domains in both sides of the wall are shown by $S_i(z_0)$ and $S_i(z_{18})(i=1, 2)$. (b) Rotation of magnetization in a 180° domain wall in NiF_2.

[14] C. Kittel, Revs. Modern Phys. **21**, 541 (1949).

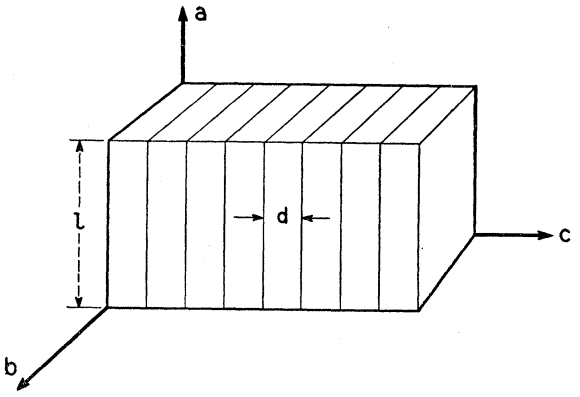

FIG. 8. A domain structure in a crystal with rectangular cross sections.

Therefore the width is of the order of

$$d\sim 0.06l^{\frac{1}{2}}\text{ cm}, \tag{9.8}$$

which is nearly two orders of magnitude larger than in the case of iron. This is due to the small magnetic moment in NiF_2.

It seems to be probable in this crystal that there are some domain boundaries related with crystal imperfections or internal strain.

10. CONCLUDING REMARKS

We studied the magnetic properties of NiF_2 theoretically with the use of a spin Hamiltonian approach which is considered to be very good in this case. Our theory seems to be consistent with almost all the data measured so far, except the neutron diffraction data by Erickson. The spin arrangement proposed by Erickson seems to be consistent neither with the fluorine nuclear resonance data nor with the torque data below the Néel temperature. Moreover, this arrangement seems not to be possible theoretically as we discussed in this paper with reference to the former work. Erickson's data on NiF_2, however, does not seem to be very accurate because of the weak intensity of magnetic scattering.

So we may say, at the present stage, that the model proposed here is reasonable. We expect further experimental studies to make the matter clearer.[15]

[15] After this paper was prepared for publication, M. Peter observed the electron spin resonance of Ni^{2+} in ZnF_2. According to his measurement, the parameter D in the spin Hamiltonian (2.1) is definitely positive. The observed values are

$$D=125.5\text{ kMc/sec }(4.19\text{ cm}^{-1}),$$
$$E=80.1\text{ kMc/sec }(2.67\text{ cm}^{-1}),$$
$$g=2.33.$$

This result also strongly supports our theory. The values of D and E estimated roughly in this paper are $D=6$ cm^{-1} and $E=1.5$ cm^{-1}, not far from the observed values. It should be noted that our estimate of D is not very accurate, because it was derived from the value of $\chi_{II}-\chi_{\perp}$ at one point of temperature. The estimate of E/J_1 may be much more accurate, but J_1 may be underestimated from T_N and θ because of the molecular field approximation. The writer wishes to thank Dr. M. Peter for informing him of his experimental result and for permitting him to quote it here prior to publication.

ACKNOWLEDGMENTS

I should like to thank Dr. R. G. Shulman for informing me of his experimental results which encouraged me to develop this work, and Dr. P. W. Anderson for reading the manuscript and kind advice on it. I also wish to thank the members of this Laboratory for their hospitality.

Note added in proof.—The behavior of the paramagnetic susceptibility near the Néel temperature is particularly noteworthy. According to the formula (3.1) in the text, $\chi_\perp$ increases very sharply near T_N and diverges at T_N, while $\chi_{\parallel}$ shows no such increase near T_N. After some manipulation (for brevity we neglect J_2 and J_3), $\chi_\perp$ in (3.1) is reduced near T_N to

$$\chi_\perp \cong [2Ng^2\mu_B^2/3k(T+\theta)]\cdot(T-T_0)/(T-T_N),$$

where

$$T_N-T_0 \cong (E^2/kJz)[(3/16)+(Jz/|\lambda|)] \cong 0.06.$$

This behavior of $\chi_\perp$ has actually been observed by Shulman (to be published) in his NMR measurement and by Cooke (private communication for which the writer wishes to thank). Burgiel, Jaccarino, and Schawlow (spoken at 1959 Cleveland Meeting) observed the same behavior in powdered NiF_2 and $Ni(IO_3)_2 2H_2O$. We can fairly generally show that this sharp increase of the magnetic susceptibility near T_N is a common feature to weak ferromagnets and the smaller the ferromagnetic moment below T_N, the sharper the increase of χ.

APPENDIX I

We shall here study the equilibrium orientation of the spins under the magnetic field using the classical spin model as in Sec. 4. We shall then calculate the torque when the magnetic field is applied in the (001), (110), and (100) planes.

The polar angles of the magnetic field **H**, the corner spin $\mathbf{S}_1$ and the body center spin $\mathbf{S}_2$ are written as (θ_0,φ_0), (θ_1,φ_1) and (θ_2,φ_2), respectively.[16] These angles are shown in Fig. 3.

The exchange, the anisotropy, and the Zeeman energies are written as follows:

$$\begin{aligned}
E_{ex} &= (N/2)8J_1S^2[\cos\theta_1\cos\theta_2 \\
&\quad +\sin\theta_1\sin\theta_2\cos(\varphi_1-\varphi_2)], \\
E_{an} &= (N/2)S^2[D(\cos^2\theta_1+\cos^2\theta_2) \\
&\quad -E(\sin^2\theta_1\cos 2\varphi_1-\sin^2\theta_2\cos 2\varphi_2)], \qquad \text{(A.1)} \\
E_z &= -(N/2)\mu_B SH[g_z\cos\theta_0(\cos\theta_1+\cos\theta_2) \\
&\quad +\sin\theta_0\cos\varphi_0(g_1\sin\theta_1\cos\varphi_1+g_2\sin\theta_2\cos\varphi_2) \\
&\quad +\sin\theta_0\sin\varphi_0(g_2\sin\theta_1\sin\varphi_1+g_1\sin\theta_2\sin\varphi_2)].
\end{aligned}$$

Putting

$$\begin{aligned}
&(\varphi_2+\varphi_1)/2=\varphi, \quad (\theta_2+\theta_1)/2=\theta, \\
&(\varphi_2-\varphi_1)/2=\psi, \quad (\theta_2-\theta_1)/2=\delta,
\end{aligned} \qquad \text{(A.2)}$$

we get

$$\begin{aligned}
\epsilon &= (E_{\text{total}}/\tfrac{1}{2}N8J_1S^2) \\
&= \cos(\theta-\delta)\cos(\theta+\delta)+\sin(\theta-\delta)\sin(\theta+\delta)\cos 2\psi \\
&\quad +\tfrac{1}{2}A_1[\cos^2(\theta-\delta)+\cos^2(\theta+\delta)] \\
&\quad -\tfrac{1}{2}A_2[\sin^2(\theta-\delta)\cos 2(\varphi-\psi)-\sin^2(\theta+\delta)\cos 2(\varphi+\psi)] \\
&\quad -\beta\{g_z\cos\theta_0[\cos(\theta-\delta)+\cos(\theta+\delta)] \\
&\quad +\sin\theta_0\cos\varphi_0[g_1\sin(\theta-\delta)\cos(\varphi-\psi) \\
&\quad +g_2\sin(\theta+\delta)\cos(\varphi+\psi)] \\
&\quad +\sin\theta_0\sin\varphi_0[g_2\sin(\theta-\delta)\sin(\varphi-\psi) \\
&\quad +g_1\sin(\theta+\delta)\sin(\varphi+\psi)]\}, \qquad \text{(A.3)}
\end{aligned}$$

where A_1 and A_2 are given by (4.4) and

$$\beta=\mu_B H/8J_1S. \qquad \text{(A.4)}$$

When the magnetic field is not large, i.e., β, β/A_1 and β/A_2 are small, the equilibrium spin orientation is very near to that with no magnetic field. So we shall take the deviation from the latter as new variables. Considering the result of Sec. 4, we write

$$\begin{aligned}
\theta &= (\pi/2)-\xi, \\
\varphi &= (\pi/4)+\eta, \qquad \text{(A.5)} \\
2\psi &= \pi-A_2-\zeta.
\end{aligned}$$

The quantities ξ, δ, η, and ζ are all expected to be small. Now we expand the energy expression (A.3) in the powers of these quantities. The expansion up to the second order with respect to ξ, δ, η, and ζ is

$$\begin{aligned}
\epsilon &= \text{const}+A\xi^2+B\delta^2+C\eta^2+D\zeta^2 \\
&\quad +X(\xi\delta+\tfrac{1}{2}\eta\zeta)+a\xi+c\eta+d\zeta, \qquad \text{(A.6)}
\end{aligned}$$

where

$$\begin{aligned}
&A=2+A_1+\tfrac{1}{2}A_2^2, \quad B=A_1+\tfrac{1}{2}A_2^2, \\
&C=2A_2^2, \quad D=\tfrac{1}{2}(1+\tfrac{1}{2}A_2^2), \\
&X=-(g_1+g_2)\beta\sin\theta_0\sin(\varphi_0-\pi/4), \\
&a=-2g_z\beta\cos\theta_0, \qquad \text{(A.7)} \\
&c=-2\beta A_2\left(\frac{g_1+g_2}{4}+\frac{8J_1}{|\lambda|}\right)\sin\theta_0\sin(\varphi_0-\pi/4), \\
&d=-\tfrac{1}{2}(g_1+g_2)\beta\sin\theta_0\cos(\varphi_0-\pi/4)+\tfrac{1}{3}A_2^3.
\end{aligned}$$

We assumed here that A_1, A_2, β/A_1, and β/A_2 are small quantities and expanded the coefficients in (A.6) in the powers of these quantities.

ξ, η, δ, and ζ are determined so as to make the energy (A.6) minimum. This is easily done and the result is as follows:

$$\begin{aligned}
&\xi=-\frac{2Ba}{4AB-X^2}, \quad \delta=\frac{Xa}{4AB-X^2}, \\
&\eta=\frac{Xd-4Dc}{8CD-\frac{1}{2}X^2}, \quad \zeta=\frac{Xc-4Cd}{8CD-\frac{1}{2}X^2}.
\end{aligned} \qquad \text{(A.8)}$$

[16] For convenience we shall take **S** parallel to the magnetic moment; **S** points the reverse direction to the true spin.

Inserting (5.7) into (5.8), we get

$$\begin{aligned}
&\xi=\tfrac{1}{2}g_z\beta\cos\theta_0,\\
&\delta=(\beta^2/8A_1)g_z(g_1+g_2)\sin2\theta_0\sin(\varphi_0-\pi/4),\\
&\eta=(\beta/2A_2)\left(\frac{g_1+g_2}{4}+\frac{8J_1}{|\lambda|}\right)\sin\theta_0\sin(\varphi_0-\pi/4),\\
&\zeta=(\beta/2)(g_1+g_2)\sin\theta_0\cos(\varphi_0-\pi/4).
\end{aligned}\tag{A.9}$$

This result is used below to calculate torques in various cases.

(1) Magnetic Field in the (001) Plane; Torque Along the c Axis

In this case $\theta_0=\pi/2$, so that

$$\begin{aligned}
&\xi=\delta=0,\\
&\eta=(\beta/2A_2)\left(\frac{g_1+g_2}{4}+\frac{8J_1}{|\lambda|}\right)\sin(\varphi_0-\pi/4),\\
&\zeta=(\beta/2)(g_1+g_2)\cos(\varphi_0-\pi/4).
\end{aligned}\tag{A.10}$$

The torque along the c axis is given by

$$\begin{aligned}
T_{[001]}=(N/2)\mu_B SH[&\sin\varphi_0(g_1\cos\varphi_1+g_2\cos\varphi_2)\\
&-\cos\varphi_0(g_2\sin\varphi_1+g_1\sin\varphi_2)].
\end{aligned}\tag{A.11}$$

Inserting (A.2), (A.5), and (A.10) into the above expression, we get

$$\begin{aligned}
T_{[001]}=N\mu_B SA_2H&\sin(\varphi_0-\pi/4)\\
&\times\left\{\left(\frac{g_1+g_2}{4}-\frac{8J_1}{|\lambda|}\right)+(3\beta/2A_2)\right.\\
&\left.\times\left[\left(\frac{g_1+g_2}{4}\right)^2+\frac{1}{3}\left(\frac{8J_1}{\lambda}\right)^2\right]\cos(\varphi_0-\pi/4)\right\}.
\end{aligned}\tag{A.12}$$

(2) Magnetic Field in the (110) Plane; Torque Along the [110] Direction

We can calculate the torque in this case in the same way as in the case (1). The result is

$$\begin{aligned}
T_{[110]}=(1/\sqrt{2})N\mu_B SA_2H&\sin\theta\\
&\times\left\{\left(\frac{g_1+g_2}{4}-\frac{8J_1}{4|\lambda|}\right)-(\sqrt{2}\beta/A_2)\right.\\
&\times\left[2(g_z/2)^2-\left(\frac{g_1+g_2}{4}\right)^2-(8J_1/16|\lambda|)\right.\\
&\left.\left.\times\left(\frac{g_1+g_2}{4}+\frac{8J_1}{|\lambda|}\right)\right]\cos\theta\right\},
\end{aligned}\tag{A.13}$$

θ being measured from the [110] direction.

(3) Magnetic Field in the (100) Plane; Torque Along the [010] Direction

We shall show only the result,

$$\begin{aligned}
T_{[010]}=NS\mu_B A_2S\sin\theta\{&[(g_1+g_2)/4]\\
&-(2\beta/A_2)[g_z{}^2-\tfrac{1}{4}(g_1+g_2)^2]\cos\theta\},
\end{aligned}\tag{A.14}$$

θ being measured from the [100] direction.

APPENDIX II

The equilibrium conditions of the spins obtained from the procedure in Sec. 6 are as follows:

$$\begin{aligned}
&\cos\theta_1\sin\theta_2\cos(\varphi_2-\varphi_1)-\sin\theta_1\cos\theta_2\\
&\quad-A_2\sin\theta_1\cos\theta_1\cos2\varphi_1-A_1\sin\theta_1\cos\theta_1\\
&+B[\cos\theta_0\sin\theta_1-\sin\theta_0\cos\theta_1\cos(\varphi_0-\varphi_1)]=0,
\end{aligned}\tag{A.15}$$

$$\begin{aligned}
&\sin\theta_2\sin(\varphi_2-\varphi_1)+A_2\sin\theta_1\sin2\varphi_1\\
&\quad-B\sin\theta_0\sin(\varphi_0-\varphi_1)=0,
\end{aligned}\tag{A.16}$$

$$\begin{aligned}
&\sin\theta_0\cos\theta_2\cos(\varphi_2-\varphi_1)-\cos\theta_1\sin\theta_2\\
&\quad+A_2\sin\theta_2\cos\theta_2\cos2\varphi_2-A_1\sin\theta_2\cos\theta_2\\
&+B[\cos\theta_0\sin\theta_2-\sin\theta_0\cos\theta_2\cos(\varphi_0-\varphi_2)]=0,
\end{aligned}\tag{A.17}$$

$$\begin{aligned}
&\sin\theta_1\sin(\varphi_2-\varphi_1)+A_2\sin\theta_2\sin2\varphi_2\\
&\quad+B\sin\theta_0\sin(\varphi_0-\varphi_2)=0.
\end{aligned}\tag{A.18}$$

APPENDIX III

The expressions of the coefficients in (6.7) are given as follows:

$$\begin{aligned}
&a=A_2\cos\theta_1\sin2\varphi_1,\\
&b=A_2\cos\theta_2\sin2\varphi_2,\\
&c=-\sin\theta_1\sin\theta_2\cos(\varphi_2-\varphi_1)-\cos\theta_1\cos\theta_2\\
&\quad-\tfrac{1}{2}A_1(3\cos^2\theta_1-1)+\tfrac{3}{2}A_2\sin^2\theta_1\cos2\varphi_1\\
&\quad+B[\cos\theta_0\cos\theta_1+\sin\theta_0\sin\theta_1\cos(\varphi_0-\varphi_1)],\\
&d=-\tfrac{1}{2}A_1\sin^2\theta_1+\tfrac{1}{2}A_2(1+\cos^2\theta_1)\cos2\varphi_1,\\
&p=(1-Ak^2)\cos\theta_2\sin(\varphi_2-\varphi_1),\\
&q=(1-Ak^2)\cos(\varphi_2-\varphi_1),\\
&r=-(1-Ak^2)[\cos\theta_1\cos\theta_2\cos(\varphi_2-\varphi_1)+\sin\theta_1\sin\theta_2],\\
&s=(1-Ak^2)\cos\theta_1\sin(\varphi_2-\varphi_1),\\
&e=-\sin\theta_1\sin\theta_2\cos(\varphi_2-\varphi_1)-\cos\theta_1\cos\theta_2\\
&\quad-\tfrac{1}{2}A_1(3\cos^2\theta_2-1)-\tfrac{3}{2}A_2\sin^2\theta_2\cos2\varphi_2\\
&\quad+B[\cos\theta_0\cos\theta_2+\sin\theta_0\sin\theta_2\cos(\varphi_0-\varphi_2)],\\
&f=-\tfrac{1}{2}A_1\sin^2\theta_2-\tfrac{1}{2}A_2(1+\cos^2\theta_2)\cos2\varphi_2.
\end{aligned}$$